# Ultra-Wideband (UWB) Positioning System Based on ESP32 and DWM3000 Modules

Sebastian Krebs
University of Applied Sciences HTWG Konstanz
Alfred-Wachtel-Str. 8, 78462 Konstanz, Germany
Email: xxx@htwg-konstanz.de

Tom Herter
University of Applied Sciences HTWG Konstanz
Alfred-Wachtel-Str. 8, 78462 Konstanz, Germany
Email: xxx@htwg-konstanz.de

***Abstract*— In this paper, we introduce an innovative Ultra-Wideband (UWB) positioning system that leverages six identical custom-designed boards, each featuring an ESP32 microcontroller and integrated with DWM3000 modules from Quorvo. This system is capable of achieving localization with an accuracy of XXX cm through Two-Way Ranging (TWR) measurements between one designated "Tag" board and five other "Anchor" boards. The collected distance measurements are processed by an Extended Kalman Filter (EKF) running locally on the Tag board, enabling it to determine its own position, relying on fixed, a priori known, positions of the Anchor boards.**
**This paper presents a comprehensive overview of the system's architecture, the key components, and the capabilities it offers for accurate indoor positioning and tracking applications.**

## I. Introduction

Indoor positioning and tracking systems gain importance in a variety of industrial fields aswell as in research [1] [2] [3] [4]. Traditional positioning systems, however, often encounter certin limitations such as meterwise accuracy [1] or a increasing positioning error [2].

In response to these challenges, Ultra-Wideband (UWB) positioning systems have emerged as a promising solution [3] [4]. Building on this technology, we have developed an UWB positioning system that utilizes hardware and advanced algorithms to generate precise position information in the three-dimensional space.

The designed UWB system consists of six identical boards, all based on the ESP32 microcontroller, a versatile and powerful platform that is oftenly used in low-cost internet of things (IoT) scenarios [5]. These custom-made printed circuit boards (PCBs) [1] are equipped with DWM3000 modules from Quorvo, which utalize powerful UWB capabilities for long-range wireless communication.

One of these boards is referred to as a "tag". It is responsible for initiating measurements with the other five "anchor" boards. The innovative aspect of the system lies in its ability to perform accurate localization without dependence on external infrastructure for centralized processing, since all the necessary calculations are performed on the device itself that is being localized.

The heart of the positioning system is the Extended Kalman Filter (EKF) implemented locally on the tag board. This EKF takes the distance measurements obtained by Two-Way Ranging (TWR) with the Anchor Boards and calculates, and, based on their a priori known positions, calculates the real-time position of the tag board with remarkable precision. The system is partially scalable; the number of anchors can be significantly increased at the expense of the general round-trip time. The ratio has the order $O(n)$.

The measuring principle of distance measurement is explained in the following section. A distance measurement was implemented based on the associated IEEE standard [7] [8]. The chapter II explains the system architecture, including the choice of anchor positions and information about the scheduled timing in relation to position measurements. This is followed by a brief description of the hardware designed and its wide range of applications as a general evaluation board. In order to explain the implementation of the firmware in more detail, chapter V describes the distribution of the functionalities to various tasks of the Real-Time Operating System (RTOS). The results of the static tests can be found in chapter VI. Both, the spatial resolution and the most important limitations are explained. Finally, the last chapter summarizes the most important findings and provides a critical review of the results.

## II. Measurement Priciple

Two-Way Ranging (TWR) is a foundational technique for obtaining precise distance measurements within the UWB positioning system. It relies on the time it takes for signals to travel from a tag board to anchor boards and back again. This time measurement, in compliance with the IEEE 802.15.4a/4z standards, offers the basis for distance estimation by multiplying the time traveled with the speed of light.

The following Figure 1 shows how a TWR Handshake is done. The Tags firmware calculates the time-of-flight (TOF) as well as the distance between both devices by comparing the timestamps of sending and reception.

For detailed technical specifications and methods, we refer interested readers to the documentation of the IEEE 802.15.4a/4z standards [7] [8], which provides comprehensive guidelines for the complex orchestration of UWB signals and the calculation of TOF. These standards ensure the correctness and accuracy of our distance measurements.

[1] layout and production files are open-source available. [6]

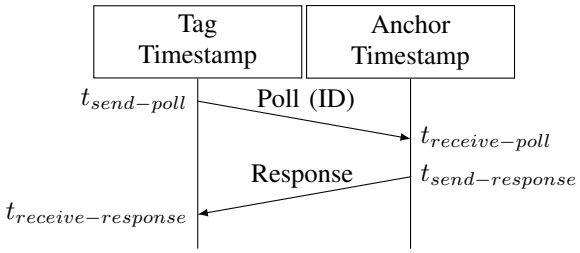


Fig. 1: Timing diagram of Two-Way Ranging (TWR)

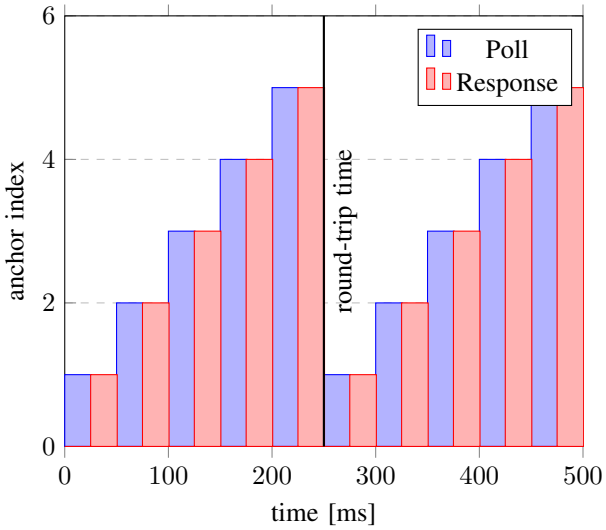


Fig. 2: Timingdiagram of the TWR measurements.

## III. System Architecture

In our scenario, five anchors are strategically distributed throughout the room, positioned at a height of 4 m on the ceiling to maximize the likelihood of Line-Of-Sight (LOS) conditions as it facilitates more accurate TOF measurements by minimizing multipath interference, and enhance signal reliability, leading to more precise and reliable location information than in an Non-Line-Of-Sight (NLOS) environment. These five anchors do not rely on information specific to their usage or mounting position.

These anchor positions are being transmitted to the tag via a Bluetooth-Low-Enegy (BLE) interface. The tag leverages these provided anchor positions, in conjunction with distance measurements, to determine its own position accurately.

The following figure 3 illustrates the interactions between the individual components.

The round-trip time of the system is the product of the number of anchors and the ranging time. The time for one distance measurement could be brought down to 50 ms per recurrence without sacrificing accuracy, leading to a general position frequency of 250 ms with 5 anchors. This low ranging time of 50 ms was achieved by implementing the firmware of the anchors interrupt-based in a multicore controller.

Detailed information about the chances taken to optimize the round-trip time by reducing each individual rangingtime

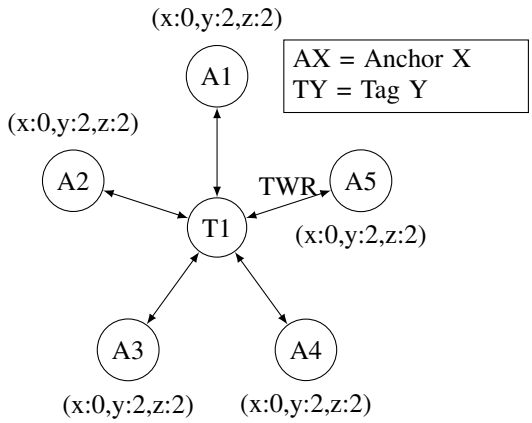


Fig. 3: System architecture for positioning.

is given in the chapter about the Firmware.

## IV. Hardware Design

The hardware design of our system draws inspiration from pre-existing DWM3000 Evaluation boards. However, our proprietary board development enables specialized component selection tailored to their intended use cases. User-friendliness was a paramount consideration during the design process, resulting in the integration of multiple user buttons and LEDs for later determined purposes like initializing the BLE server and entering the configuration mode to change the stored anchor positions. Additionally, the PCB incorporates a convenient LiPo battery charging capability via USB-C.

Notably, our PCB design ensures a consistent layout across all boards, regardless of their specific application. Below the antennas of both the DWM3000 and ESP32, the ground plate has been selectively omitted to enhance antenna radiation characteristics and enable more precise measurements. This meticulous hardware design approach not only optimizes performance but also prioritizes user convenience.

## V. Firmware Architecture

To meet the demanding timing requirements essential for TOF measurements and enhance network round-trip times, our firmware is implemented based on a RTOS. In particular FreeRTOS [9] offers the capability to create multiple tasks that collaborate coherently and can be executed simultaneously on each of the two cores of the ESP32 microcontroller.

The documentation of the source code is continuously made available online with the help of Doxygen and GitHub pages. The implementation can therefore be viewed publicly [10].

In the regular tracking mode, all devices within the system execute the TOF task, ensuring synchronized data acquisition. When a device is configured as a tag, it additionally undertakes the execution of the EKF task. The EKF task processes the distance measurements generated by the TOF task, culminating in a precise positional estimation.

### A. TOF-Task

The TOF task in our system is based on the example code provided by Quorvo for TWR measurements. However, we have refined the functionality by structuring it in a class-based framework. The commonalities between the Initiator and Responder roles have been encapsulated in a common superclass. This design decision allows us to maintain a lean and clear software structure, reduce redundancy and simplify maintenance.

In practice, the tag, which acts as the TWR initiator, as part ov the localization architecture iterates through a list of anchors, each of which serves as an individual TWR responder. The tag generates distance measurements with each anchor. The result is a comprehensive data set that serves as the basis for precise localization calculation.

### B. EKF-Task

The EKF employed in our system leverages two distinct mathematical models to achieve precise position estimation. For readers interested in delving deeper into the theoretical foundations of the Kalman Filter, we recommend consulting the work of Li Qiang et al. in "Kalman Filter and Its Application" [11]. The EKF on the tag utilizes a prediction model based on the constant velocity and trajectory model assumption.

This model serves as a fundamental tool for forecasting the future position of the tag. For potentially more dynamic systems the use of more realistic models for the tag movement could improve the dynamic behavior of the Kalman Filter.

The measurement model is encapsulated in the Jacobian matrix given, in Equation 1, enabling the transformation of measured distances into accurate position estimations. The measurement model finds its expression in the measurement matrix $H$, which effectively links the measured distances to the position estimation:

$$\begin{aligned} \Delta x_i &= x_i - x \\ \Delta y_i &= y_i - y \\ \Delta z_i &= z_i - z \\ dist_i &= \sqrt{\Delta x_i^2 + \Delta y_i^2 + \Delta z_i^2} \\ H &= \begin{bmatrix} -\frac{\Delta x_1}{dist_1} & -\frac{\Delta y_1}{dist_1} & -\frac{\Delta z_1}{dist_1} \\ -\frac{\Delta x_2}{dist_2} & -\frac{\Delta y_2}{dist_2} & -\frac{\Delta z_2}{dist_2} \\ \vdots & \vdots & \vdots \\ -\frac{\Delta x_{\max}}{dist_{\max}} & -\frac{\Delta y_{\max}}{dist_{\max}} & -\frac{\Delta z_{\max}}{dist_{\max}} \end{bmatrix} \end{aligned} \tag{1}$$

By using the matrix $H$, the EKF is able to directly translate the position estimate into predicted distance measurements. These are further compared to real distance measurements and based on this information the position estimate is improved.

## VI. Test Results

The implementation of localization systems often requires the evaluation of the measured values through empirical, static and dynamic tests. Since the dynamics of position determination are largely determined by the parameterization of the EKF, a detailed evaluation of the system's ability to detect moving objects is omitted.

Static tests were carried out. The effect of the anchor arrangement is crucial to the success of the system. In the case of these tests, the anchors were mounted at a height of 4m. One single anchor was mounted at a height of 1m to ensure good position resolution in the Z axis. Otherwise, an overestimation of the distances and, thus, a poor calculation of the Z axis was determined.

During testing, attention was paid to keep LOS conditions, although tests showed that the influence of NLOS conditions can be partially compensated for by using the EKF. The table below shows fixed positions in the room that were measured using the system over a fixed period of time to make them comparable to each other. To do this, the mean deviation and the fluctuation of the values over the standard deviation are then considered and evaluated.

| **Position[m]** | $\mu$**[cm]** | $\sigma$**[cm]** |
|---|---|---|
| $(x, y)$ | $mean(length)$ | $std(length)$ |
| $(2.0, 2.0)$ | $67.66cm$ | $2.90cm$ |
| $(2.0, 3.0)$ | $55.42cm$ | $2.97cm$ |
| $(2.0, 4.0)$ | $65.05cm$ | $2.8cm$ |
| $(2.0, 5.0)$ | $47.31cm$ | $3.51cm$ |
| $(2.0, 6.0)$ | $46.07cm$ | $3.13cm$ |
| $(2.0, 7.0)$ | $54.00cm$ | $3.17cm$ |
| $(2.0, 8.0)$ | $34.48cm$ | $3.3cm$ |
| $(3.0, 2.0)$ | $31.74cm$ | $3.42cm$ |
| $(3.0, 3.0)$ | $121.37cm$ | $4.47cm$ |
| $(3.0, 4.0)$ | $23.06cm$ | $3.07cm$ |
| $(3.0, 5.0)$ | $29.34cm$ | $2.91cm$ |
| $(3.0, 6.0)$ | $28.31cm$ | $2.93cm$ |
| $(3.0, 7.0)$ | $22.68cm$ | $3.2cm$ |
| $(3.0, 8.0)$ | $32.98cm$ | $3.73cm$ |
| $(4.0, 2.0)$ | $19.75cm$ | $2.97cm$ |
| $(4.0, 3.0)$ | $21.73cm$ | $3.4cm$ |
| $(4.0, 4.0)$ | $29.91cm$ | $2.9cm$ |
| $(4.0, 5.0)$ | $9.27cm$ | $3.2cm$ |
| $(4.0, 6.0)$ | $28.1cm$ | $2.84cm$ |
| $(4.0, 7.0)$ | $35.95cm$ | $8.34cm$ |
| $(4.0, 8.0)$ | $14.88cm$ | $3.13cm$ |
| $(5.0, 2.0)$ | $80.12cm$ | $3.61cm$ |
| $(5.0, 3.0)$ | $61.88cm$ | $4.19cm$ |
| $(5.0, 4.0)$ | $47.44cm$ | $3.57cm$ |
| $(5.0, 5.0)$ | $21.28cm$ | $6.76cm$ |
| $(5.0, 6.0)$ | $31.89cm$ | $3.65cm$ |
| $(5.0, 7.0)$ | $33.02cm$ | $3.72cm$ |
| $(5.0, 8.0)$ | $26.27cm$ | $3.73cm$ |
| $(6.0, 2.0)$ | $89.12cm$ | $2.99cm$ |
| $(6.0, 3.0)$ | $99.28cm$ | $4.28cm$ |
| $(6.0, 4.0)$ | $73.01cm$ | $3.88cm$ |
| $(6.0, 5.0)$ | $55.42cm$ | $6.16cm$ |
| $(6.0, 6.0)$ | $10.63cm$ | $4.56cm$ |
| $(6.0, 7.0)$ | $29.46cm$ | $7.01cm$ |
| $(6.0, 8.0)$ | $13.0cm$ | $2.86cm$ |

TABLE I: Static mesurement deviation out of 500 measurements

Because position-related changes in accuracy were determined during the test, a grid-based measurement was carried out in addition to the static test. The 10 mx8 m room was divided into 1 mx1 m squares using a grid. Multiple measurement was then carried out over the course of three minutes at each grid intersection point. This procedure allows the deviations of the positions to be represented in relation to the

location in the room. For the following illustration, $\sigma$-ellipses were drawn to show the scattering per position.

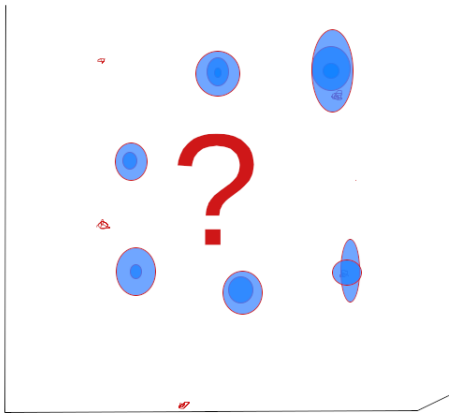

Fig. 4: Position deviation per coordinates in the room.

As can be seen from the figure 4, significant deviations were recorded outside the area enclosed by the anchors. Even if the system is clearly capable of very precise positioning, it can be said that if uniform positioning accuracy is to be achieved, the best arrangement of the anchors must be determined using simulation means. This ensures that the propabillity of occuring ”blind spots” is reduced.

## VII. Conclusion And Outlook

In conclusion, it can be said that a very precise localization system has been designed. Both the hardware and the software were designed specifically for use as a positioning module and fulfill this purpose with a satisfying accuracy of XXX (noch einfügen und ggf. erläutern wo besser wo schlechter).

A critical point is that the system’s is scalability has a linear impact on its temporal performance. By pinging every single anchor, the tag is not able to handle a very large number of anchors without increasing the roundtrip time. This problem could be avoided by instead of TWR measurements Time-difference-of-Arrival (TdoA) measurements would be performed. Even if this measurement principle requires a nanosecond precise synchronization of the anchors, the roundtrip time would be limited to the duration of one ping process.

Initially, a hybrid solution using TWR and TdoA measurements was planned, but the wireless clock synchronization of the anchors is currently only possible with limited accuracy. Further research in this area could allow the system to generate accurate position measurements with a period duration of up to 50ms.

## References


[1] S. M. Kouhini, C. Kottke, Z. Ma, R. Freund, V. Jungnickel, M. Müller, D. Behnke, M. M. Vazquez, and J.-P. M. G. Linnartz, “Lifi positioning for industry 4.0,” *IEEE Journal of Selected Topics in Quantum Electronics*, vol. 27, no. 6, pp. 1–15, 2021.

[2] H. Liu and G. Pang, “Accelerometer for mobile robot positioning,” *IEEE Transactions on Industry Applications*, vol. 37, no. 3, pp. 812–819, 2001.

[3] G. Schroeer, “A real-time uwb multi-channel indoor positioning system for industrial scenarios,” in *2018 International Conference on Indoor Positioning and Indoor Navigation (IPIN)*, 2018, pp. 1–5.

[4] Y. Xianjia, L. Qingqing, J. P. Queralta, J. Heikkonen, and T. Westerlund, “Applications of uwb networks and positioning to autonomous robots and industrial systems,” in *2021 10th Mediterranean Conference on Embedded Computing (MECO)*, 2021, pp. 1–6.

[5] M. Babiuch, P. Foltýnek, and P. Smutný, “Using the esp32 microcontroller for data processing,” in *2019 20th International Carpathian Control Conference (ICCC)*, 2019, pp. 1–6.

[6] S. Krebs and T. Herter, “uwb-tracking,” https://github.com/krebsbstn/uwb-tracking, 2023.

[7] “IEEE-standard 802.15.4a-2007: Part 15.4: Wireless Medium Access Control (MAC) and Physical Layer (PHY) Specifications for Low-Rate Wireless Personal Area Networks (LR-WPANs): Amendment 1: Add Alternate PHYs,” 2007.

[8] “IEEE-Standard 802.15.4z-2020: Part 15.4: Wireless Medium Access Control (MAC) and Physical Layer (PHY) Specifications for Low-Rate Wireless Personal Area Networks (LR-WPANs): Amendment 6: Ultrawideband PHYs,” 2020.

[9] Aug 2023. [Online]. Available: https://www.freertos.org/index.html

[10] S. Krebs and T. Herter, November 2023. [Online]. Available: https://krebsbstn.github.io/uwb-tracking/files.html

[11] Q. Li, R. Li, K. Ji, and W. Dai, “Kalman filter and its application,” in *2015 8th International Conference on Intelligent Networks and Intelligent Systems (ICINIS)*, 2015, pp. 74–77.